Asian Journal of Chemistry; Vol. 34, No. 10 (2022), 2623-2632

ASIAN JOURNAL OF CHEMISTRY

https://doi.org/10.14233/ajchem.2022.23865

DFT, Molecular Docking, Toxicity Investigations and Antifungal Efficacy of *N*-Aryl Amides of Pyrido[1,2-*a*]pyrimidin-2-one

ABINAYA ANBAZHAGAN and SHARULATHA VENUGOPAL*

Department of Chemistry, Avinashilingam Institute for Home Science and Higher Education for Women, Coimbatore-641043, India

*Corresponding author: E-mail: sharulatha_chem@avinuty.ac.in

Received: 8 April 2022; *Accepted*: 23 June 2022; *Published online*: 19 September 2022; AJC-20965

Potent kinase inhibitors containing *N*-aryl bonds play a crucial role for enzyme inhibition. Hence, the present investigation was carried out to evaluate the antifungal activity of *N*-aryl amides of pyrido[1,2-*a*]pyrimidin 2-ones. The synthesized compounds were evaluated for their *in vitro* antifungal activity against *Aspergillus niger* and *Candida albicans* by the disc diffusion method. All the compounds showed significant antifungal activity. Further, the docking studies were carried out against the active site of 1NMT and 1KS5 fungi protein. The whole compounds showed great binding affinity and possess bioavailability. DFT/B3LYP technique using the 6-31G basis set at gaseous phase all the compounds were optimized and the HOMO-LUMO energies also calculated. Furthermore, *in silico* prediction of toxicity and bioactive score values indicates that the compounds are highly reactive. According to Lipinski's "rule of five," all the compounds are expected to be biologically active. It is expected that these findings will provide clarity regarding molecular recognition and will undoubtedly aid drug scientists in developing novel drugs in the future.

Keywords: Pyridopyrimidine, Antifungal Activity, Molecular docking, DFT, Toxicity, Molecular properties.

INTRODUCTION

One of medicinal chemistry's greatest achivements has been in the fight against fungal infection. The only medicine available to cure major fungal infections was amphotericin, which is known to cause considerable nephrotoxicity. The approval of imidazoles and triazoles in the late 1980s marked a significant improvement to treat local and systemic fungal infections safely and efficiently [1]. These developments and the associated increase in fungal infections intensified the search for new, safer and more effacious agents to combat serious fungal infections.

Pyridopyrimidine is a fascinating heterocyclic moiety that has high antifungal activity and is made up of a number of physiologically active compounds [2]. The pyridopyrimidine ring's polar nitrogen atom promotes bioactivity to compounds and facilitates their interaction with macromolecules [3]. Its derivatives have long been used in the synthesis of medicinal intermediates. With the various therapeutic properties of the pyridopyrimidine ring in mind, it is decided to synthesize a number of compounds with nitrogen as core element and assays them *in vitro* for antifungal activity [4]. Biological effects of amide derivatives include anticancer, antihistamine, antifungal, and antibacterial activities. Many potent kinase inhibitors containing *N*-aryl bonds play a crucial role for enzyme inhibition as observed in the case of imatinib and ZM-447439 [5].

Designing of drugs for various diseases necessitates theoretical modeling of the drug's structure. Rather than synthesizing the appropriate compounds for treatment, researchers prefer to design the structure of drugs using theoretical modeling. One such method is molecular docking, which involves checking the interaction of drugs with the appropriate proteins [6]. Molecular docking is a computational method for predicting the binding of bioactive compounds to specific proteins or for predicting the target proteins for one bioactive compound [7]. In drug design industry, molecular docking is an effective strategy for gaining insight into ligand-receptor interactions. Molecular docking plays a significant role in drug development due its ability to predict the best binding mode between drugs and the target protein [8].

N-Aryl amides derivatives were synthesized in prior investigations and some of the compounds exhibited potential

antibacterial activity against phytopathogens [9]. In continuation of our research, the current work evaluates the antifungal efficacy of *N*-aryl amides of pyrido[1,2-*a*]pyrimidin 2-ones as well as *in silico* analyses such as molecular docking, DFT, toxicity, bioactive score and ADME property.

EXPERIMENTAL

N-Aryl amides derivatives were synthesized according to the reported procedure [9] and used for the antifungal activity.

Antifungal activity: The disc diffusion method was used to assess the synthesized compounds for antifungal activity against *Aspergillus niger* and *Candida albicans* fungal strains *in vitro* against the standard clotrimazole drug (10 g/disc). Each Petri plate was divided into four quadrants, with I (100 mcg), II (200 mcg) and III (300mcg) discs extracted in three quadrants (discs are soaked overnight in extract solution). Using sterile forceps, one quadrant of standard Clotrimazole 5 mcg was inserted in each quadrant. Petri dishes were set for 1 h of diffusion in the refrigerator at 40 ºC at room temperature [10] followed by incubation for 24 to 48 h at room temperature. The zone of inhibition was measured and then the average of two measurements was recorded.

Molecular docking: *N*-Aryl amides derivatives (**A-H**) with strong experimental antifungal activity point to the need for molecular docking studies to identify a viable target usingAutodock vina 1.5.6 software. ChemDraw Ultra 12.0 was used to draw the structure of synthesized molecules and Gaussian Software 16W was used to optimize the structure [11,12]. The ligand was then generated into PDBQT using the graphical interface programme MGL tools. *endo*-1, 4-Glucanase (PDB id: 1KS5) [10,13-15] and *N*-myristoyltransferase (PDB id: 1NMT) [16-20] from the protein data bank coordinate file were used as antifungal receptor molecules. The grid box was customized using MGL tools in order to execute docking simulations. Autodock Vina was used to find the optimal docked conformation for compounds with proteins as well as their binding affinity. The visual description of the interaction between the ligands and the target protein was deduced using LigPlot+ and PyMol. The 3D coordinates of the target receptor were derived using the 1KS5 and 1NMT -Proteins, and the optimum docked conformation of the tested structures was identified using glide energy, binding energy, active hydrogen bonding sites, and hydrophobic interactions [21].

Toxicity potential prediction: Toxicity risk prediction provides an insight into the potential negative effects of synthesized molecules that could be utilized in drug development and discovery. A pre-computed series of structural fragments was used to assess mutagenic, tumorigenic, irritant and reproductive toxicity [22]. OSIRIS Property Explorer Software was performed to create toxic parameters for the synthesized compound [23].

Bioactivity score assessment: Drug score values show compound's overall potential as a drug candidate. Molinspiration cheminformatic software is a web-based application that predicts the bioactivity of synthesized compounds against common human receptors such G protein-coupled receptors (GPCR) ligands, ion channels, kinases, nuclear receptors, proteases and enzymes [23].

Lipinski's Rule of five: Lipinski's rule of five is useful for characterizing the molecular features of drug molecules that are needed to assess critical pharmacokinetic parameters like absorption, distribution, metabolism, excretion and toxicity (ADMET). The rule is useful in therapeutic development and design. *in silico*, ADMET analysis can predict several significant traits and it is useful for evaluating a molecule's desirable attributes. The current study evaluates ADMET properties such as aqueous solubility (log S), skin permeability (log K_p), lipophilicity, percentage absorption, pharmacokinetics and drug-likeness properties of small molecules using an online portal called SwissADME [24,25].

Computational methods: For the investigated compounds, full geometry optimizations were performed utilizing the DFT at the B3LYP level using Gaussian 16w software. The 6-31G basis set level was used to compute the properties and HOMO-LUMO energies of the investigated compounds. At the same level of approach, Mulliken charge distributions, molecular electro static potential, natural bond analyses and quantum chemical parameters were computed [10]. Gaussian programme output files were viewed using Gaussian view 6.1.

RESULTS AND DISCUSSION

Antifungal activity: The disc diffusion method was used to evaluate the *in vitro* antifungal activity of the synthesized *N*-aryl amides derivatives (**A-H**) against *Aspergillus niger* and *Candida albicans* and compared with clotrimazole (10 g/disc) as a reference. According to study, *N*-aryl amides derivatives (**A-H**) had antifungal activity agai*nst A. niger* and *C. albicans* in zones ranging from 17-23 mm for *A. niger* and 15-30 mm for *C. albicans* (Fig. 1).

The inhibitory results at three different concentrations, 50 g, 100 g and 150 g demonstrated that *N*-aryl amides derivatives are susceptible to fungus at higher concentrations, but not so much at lower concentrations. The growth percentage in comparison to the control was calculated using the formula below, where the control's growth percentage was 100%.

$$\text{Growth (\%)} = \frac{\text{Growth of fungi with compound}}{\text{Growth of fungi with control}} \times 100$$

The antifungal analysis was also assessed in terms of growth percentage compared to the control, where the control's growth is 100%, using the formula below, which reveals the compound's ability to exhibit potency against any fungal stain [10].

$$\text{Inhibition (\%)} = \text{Control}_{\text{Growth percentage}} - \text{Compound}_{\text{Growth percentage}}$$

Compounds **C**, **E** and **H** improved the sensitivity against *A. niger* and *C. albicans*, as indicated in Table-1, with compounds **C** and **H** displaying the most action since both the molecules have chlorine atom [10], whereas the enhanced activity of compound **E** is due the presence of more reactive naphthalene ring. In both fungal strains, compounds **A** and **D** had the least level of activity. Inhibition of fungal growth by the reported compounds, indicate the compounds' broad-spectrum antifungal potentials, which make the synthesized compounds for bioprospecting for antibiotic drugs.

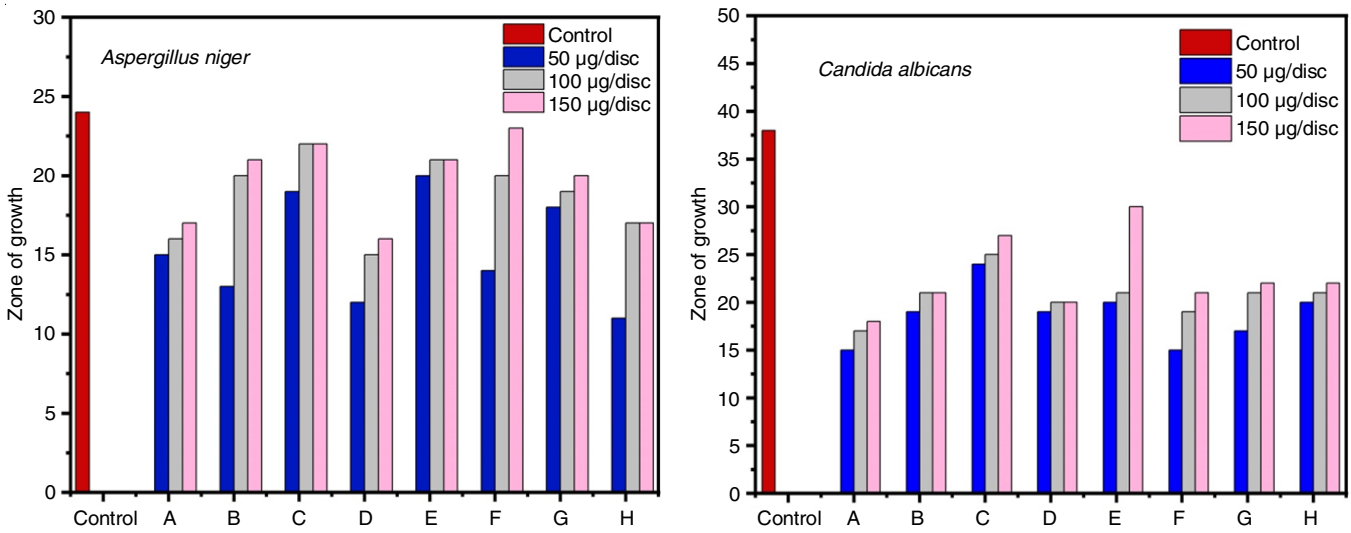

Fig. 1. Zone of growth plot of synthesized compounds (**A-H**) against *Aspergillus niger* and *Candida albicans* tested by disc diffusion assay

TABLE-1
DATA OF PERCENTAGE GROWTH AND INHIBITION AGAINST *Aspergillus niger* AND *Candida albicans*

Compd.	*Aspergillus niger*						*Candida albicans*					
	50 µg/disc		100 µg/disc		150 µg/disc		50 µg/disc		100 µg/disc		150 µg/disc	
	Growth (%)	Inh. (%)	Growth (%)	Inh. (%)	Growth (%)	Inh. (%)	Growth (%)	Inh. (%)	Growth (%)	Inh. (%)	Growth (%)	Inh. (%)
Control	100%	0%	100%	0%	100%	0%	100%	0%	100%	0%	100%	0%
A	62.50	37.50	66.66	33.34	70.83	29.17	39.47	60.53	44.73	55.27	47.36	52.64
B	54.15	45.85	83.33	16.67	87.50	12.50	50.00	50.00	55.26	44.26	55.26	44.26
C	79.16	20.84	91.66	8.34	91.66	8.34	63.15	36.85	65.78	34.22	71.05	28.95
D	50.00	50.00	62.50	37.50	66.66	33.34	50.00	50.00	52.63	47.37	52.63	47.37
E	83.33	16.67	87.50	12.50	87.50	12.50	52.63	47.37	55.26	44.74	78.94	21.06
F	58.33	41.67	83.33	16.67	95.83	4.17	39.47	60.53	50.00	50.00	55.26	44.74
G	75.00	25.00	79.16	20.84	83.33	16.67	44.73	55.27	55.26	44.74	57.89	42.11
H	45.83	54.17	70.83	29.17	70.83	29.17	52.63	47.37	55.26	44.74	57.89	42.11

Molecular docking: The N-myristoyltransferase (1NMT) is essential for viability in a number of human pathogens, including the fungi, *Candida albicans*, which is important in a variety of biological processes with signal transduction pathways, apoptosis [16,18] and significant for the growth of fungal cells [19,20]. *Aspergillus niger* as a mammalian pathogen can secrete large amounts of different cellulases, in which *endo*-1,4-glucanase(1KS5) [15] is the main component which cleave the internal β-1,4-glucosidic bonds to cellooligosaccharides and responsible for the biosynthesis and remodelling the fungi cell wall [26]. As a result, inhibiting these proteins prevents biosynthesis, affecting the cell wall's integrity and consequently leading to the cell death.

Furthermore, the docking interactions between these fugal proteins 1NMT and 1KS5 and the synthesized compounds (A-H) was carried out to identify the most significantly interacting residues and the type of thermodynamic interactions responsible for the binding of these molecules. The docking run produced nine distinct positions for each compound, along with the appropriate binding energy scores; the best-docked poses with the lowest energy from a total of nine poses for each compound were retained. Tables 2 and 3 show the docking findings of the investigated drugs. Fig. 2 illustrate the 2D and 3D depictions of *N*-aryl amides derivatives (**A-H**) interacting with the target receptors 1KS5 and 1NMT, respectively. According to the findings, the investigated compounds interacted extensively with amino acids of the target proteins 1KS5 and 1NMT, with binding energies ranging from -9.7 to -7.5 kcal/mol, which is superior to the binding energy of the conventional drug clotrimazole.

Compound **E** was shown to have the best docking binding energies of -9.6 and -9.7 kcal/mol with the target receptors 1KS5 and 1NMT through three conventional hydrogen bonds [Gln200A-2.89 Å, Asn20A-3.61 Å, Asn63A-3.91 Å and Asp170B-3.01 Å, Pro190A-3.59 Å, Lys194A-3.98 Å], since it contains more reactive naphthalene group attachment. The compounds also had the greatest hydrophobic interactions (six) with the target proteins. This orientation in terms of hydrogen bonding and hydrophobic interactions could help antifungal activity. As a result, *N*-aryl amides derivatives (**A-H**) may be effective at interacting with the target receptor, indicating that the molecules under investigation are biologically active.

Toxicity potential prediction: The toxicity risk predictor looks for fragments in a molecule that could indicate toxicity. The findings clearly revealed that all *N*-aryl amides derivatives (**A-H**), with the exception of compound **E**, are safe and likely

TABLE-2
PREDICTED H-BONDS, H-BOND LENGTH, H-HYDROPHOBIC INTERACTIONS, BINDING ENERGY (kcal/mol) BETWEEN LIGANDS (A-H) AND MACROMOLECULE *Aspergillus niger* (PDB-1KS5)

Compounds	Hydrogen bonds	H-Bond length (Å)	H-bond with	Hydrophobic Interactions	Binding energy (kcal/mol)
A	3	2.80, 3.27, 3.55	Asn63(A), Gln200(A), Asn20(A)	Tyr7(A), Asn20(A), Tyr61(A)	-7.5
B	3	2.79, 3.32, 3.37	Asn63(A), Gln200(A), Asn20(A)	Asn20(A), Tyr61(A), Trp22(A)	-8.0
C	3	3.18, 3.23, 3.98	Asn63(A), Gln200(A), Asn20(A)	Asn20(A), Tyr61(A)	-7.9
D	4	2.91, 3.40, 3.41, 3.80	Gln200(A), Glu204(A), Asn20(A), Asn63(A)	Asn20(A), Trp22(A)	-8.1
E	3	2.89, 3.61, 3.91	Gln200(A), Asn20(A), Asn63(A)	Asn20(A), Tyr61(A), Tyr7(A), Trp22(A)	-9.6
F	3	2.92, 3.53, 3.85	Gln200(A), Asn20(A), Asn63(A)	Asn20(A), Tyr61(A), Tyr7(A), Trp22(A)	-8.7
G	4	2.92, 3.36, 3.48, 3.90	Gln200(A), Glu204(A), Asn20(A), Asn63(A)	Asn20(A), Tyr61(A), Tyr7(A), Trp22(A)	-8.4
H	3	3.23, 3.25, 3.88	Ser111(A), Gln200(A), Asn20(A)	Asn18(A), Tyr7(A), Trp22(A), Phe101(A)	-8.3
Std. (S)	3	2.94, 3.23, 3.67	Asn20(A), Asn63(A), Gln200(A)	Asn20(A), Tyr7(A),	-6.5

TABLE-3
PREDICTED H-BONDS, H-BOND LENGTH, H-HYDROPHOBIC INTERACTIONS, BINDING ENERGY (kcal/mol) BETWEEN LIGANDS (A-H) AND MACROMOLECULE *Candida albicans* (PDB-1NMT)

Compounds	Hydrogen bonds	H-Bond length (Å)	H-bond with	Hydrophobic Interactions	Binding energy (kcal/mol)
A	5	2.80, 3.72, 4.00, 4.06, 4.10	Gln207(B), Asp170(B), Gln207(B), Asp170(B), Trp206(B)	Pro62(B), Leu66(B), Asp170(B), Pro190(A), Val191(A), Ile205(B)	-8.3
B	3	3.19, 3.72, 4.09	Lys284(C), Lys436(B) Ser280(C)	Pro219(B), Tyr283(C), Phe414(B)	-8.6
C	4	2.80, 3.25, 3.54, 3.91	Glu109(B), Gly213(B), Ser214(B), Tyr210(B)	Leu415(B)	-8.4
D	2	3.03, 3.31	Thr197(B), Asn201(B)	Pro217(B), Leu216(B), Thr197(B), Val168(C), Ile193(B), Leu294(C), Phe420(B)	-8.0
E	3	3.01, 3.59, 3.98	Asp170(B), Pro190(A), Lys194(A)	Leu216(A), Val168(B), Ile193(B), Leu294(C), Phe420(B), Ile169(B),	-9.7
F	3	3.09, 3.22, 3.96	Lys284(C), Lys436(B) Ser280(C)	Pro219(B), Phe414(B)	-8.9
G	2	3.09, 3.23	Thr197(B), Asn201(B)	Val168(B), Ile193(B), Leu294(C), Phe420(B), Pro217(B), Thr197(B)	-8.3
H	3	2.99, 3.92, 3.98	Lys436(B), Lys284(C), Ser280(C)	Ile215(B), Phe414(B), Thr222(B), Tyr283(C), Lys284(C)	-8.6
Std. (S)	2	3.33, 3.84	Asp64(B), Val168(C)	Ile63(B), Val168(C), Thr197(B), Phe420(B)	-7.5

to have almost no toxicity in terms of mutagenicity, tumorigenicity, irritant and reproductive system effects. According to Table-4, all of the compounds performed well in screening, with the best drug score values (DS = 0.870.85), with the exception of compound **E**, which had lower values (DS = 0.32).

Bioactivity score assessment: Different characteristics such as binding to G protein-coupled receptor (GPCR) ligand and nuclear receptor ligand, ion channel modulation, kinase inhibition, protease inhibition and enzyme activity inhibition were used to compute the bioactivity scores of the synthesized compounds. All of the parameters were estimated using the online software Molinspiration, which projected that the synthesized compounds would have significant biological activity. The bioactivity score is given in Table-5. It is known that if the bioactivity score for molecules is greater than 0.0, the group is active; if it is between -5.0 and 0.0, the molecule is moderately

TABLE-4
TOXIC POTENTIALITY OF THE SYNTHESIZED COMPOUNDS (**A-H**)

Compounds	Toxic potentiality (K_i or IC_{50} in nmol/L)				
	Mutagenic	Tumorigenic	Reproductive	Irritant	Drug score None < 0.8 < High
A	None	None	None	None	0.867
B	None	None	None	None	0.861
C	None	None	None	None	0.874
D	None	None	None	None	0.875
E	Medium	High	None	None	0.326
F	None	None	None	None	0.861
G	None	None	None	None	0.873
H	None	None	None	None	0.857

	2D representation of the compounds (A-H) with *Aspergillus niger* (PDB-1 KS5)	3D representation of the compounds (A-H) with *Aspergillus niger* (PDB- 1KS5)	2D representation of the compounds (A-H) with *Candida albicans* (PDB-1NMT)	3D representation of the compounds (A-H) with *Candida albicans* (PDB-1NMT)
A	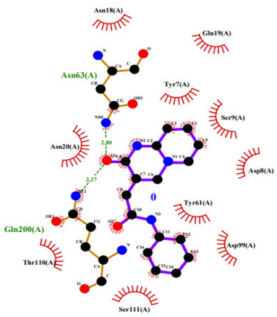	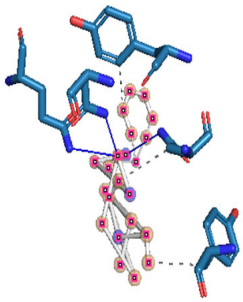	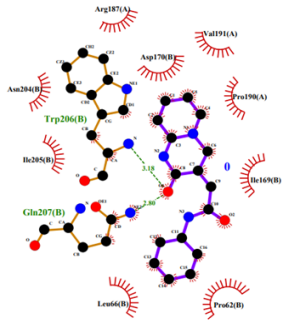	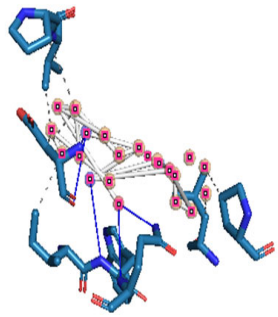
B	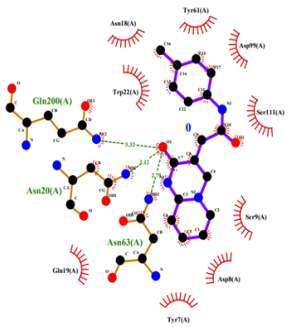	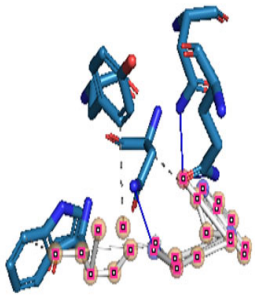	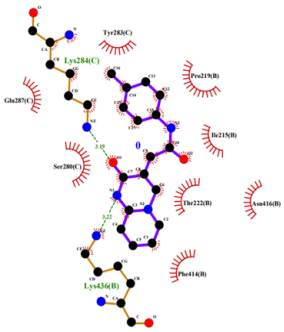	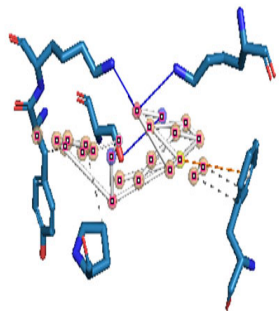
C	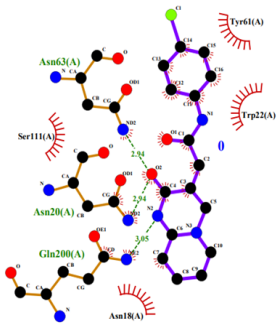	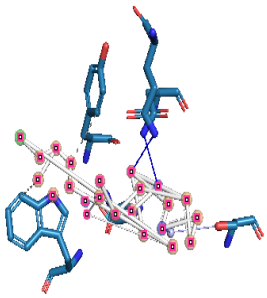	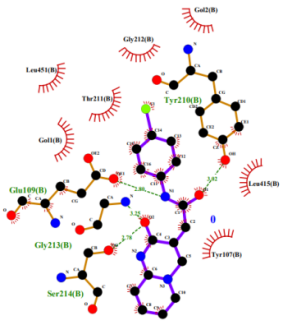	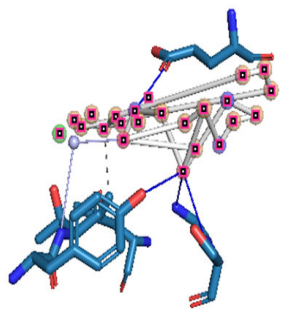
D	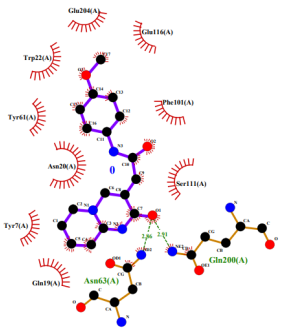	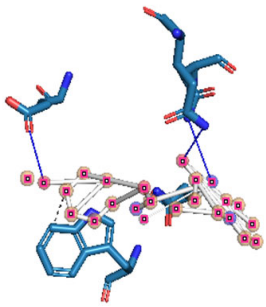	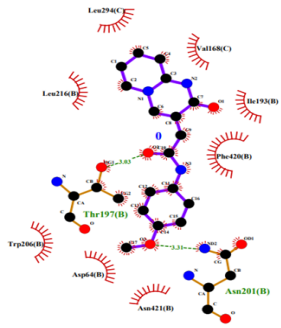	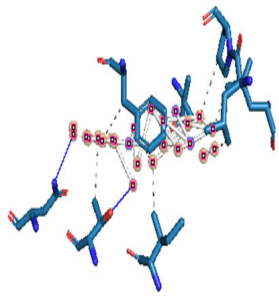
E	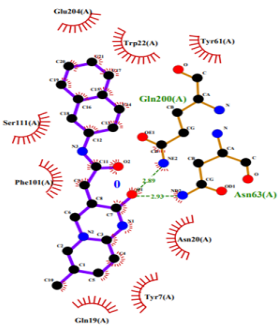	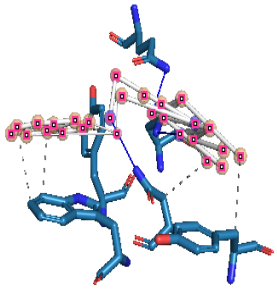	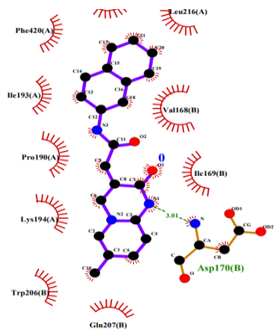	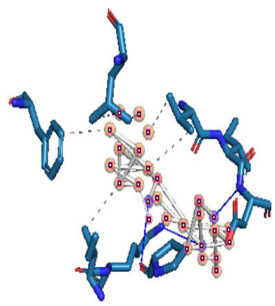

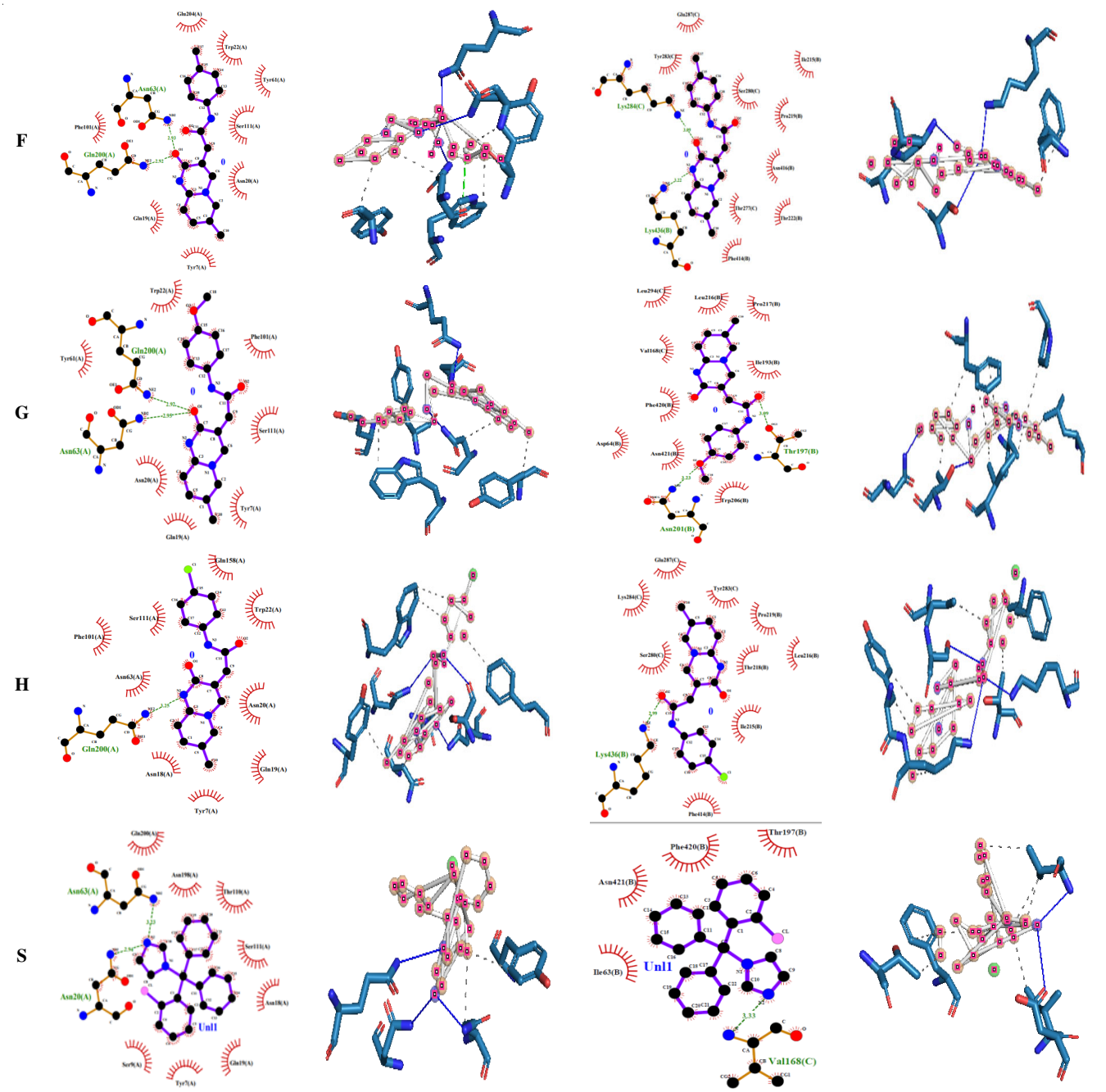

Fig. 2. 2D and 3D representation of the interaction of the compounds (**A-H**) with macromolecule *Aspergillus niger* (PDB-1KS5) and *Candida albicans* (PDB-1NMT)

TABLE-5
BIOACTIVITY SCORE OF THE SYNTHESIZED COMPOUNDS (**A-H**)

Compounds	Parameters of bioactivity score					
	GPCR ligand	Ion channel modulator	Kinase inhibitor	Nuclear receptor ligand	Protease inhibitor	Enzyme inhibitor
A	-0.49	-0.59	-0.58	-0.77	-0.71	-0.42
B	-0.49	-0.66	-0.58	-0.74	-0.71	-0.48
C	-0.45	-0.57	-0.55	-0.74	-0.69	-0.45
D	-0.46	-0.63	-0.54	-0.68	-0.65	-0.44
E	-0.34	-0.54	-0.44	-0.62	-0.56	-0.35
F	-0.47	-0.67	-0.59	-0.77	-0.73	-0.47
G	-0.47	-0.67	-0.58	-0.73	-0.72	-0.48
H	-0.45	-0.65	-0.59	-0.77	-0.76	-0.48

active; and if it is less than -5.0, the product is inert [23]. The bioactivity scores of *N*-aryl amides derivatives (**A-H**) ranged from -5.0 to 0.0, among the entire, compound **E** exhibits higher values (-0.46, -0.63, -0.54, -0.68, -0.65 -0.44) which intimates that compound **E** is more active molecule then the others, and can behave as potential drugs with minor chemical modifications.

Lipinski's rule of five: The absorption, distribution, metabolism and excretion (ADME) of a drug in the human body provides the information about the oral absorption or membrane permeability of the evaluated molecule using various rules such as Lipinski's rule of five, which states that compounds with good membrane permeability should have MW ≤ 500, RB ≤ 10, ClogP ≤ 5 , HBA ≤ 10 and HBD ≤ 5 [27]. All of the compounds satisfied Lipinski's rule and the values of molecular properties are tabulated in Table-6. The value of molar refractivity of the studied compounds lies within its range *i.e*. 40-130 similarly the value of TPSA of all the studied compound lies in the range 63.46-72.69 Å^2, which is under the 140 Å^2 upper limit of TPSA [28]. All the compounds show high GI absorption, whereas compounds **D** and **G** are not available for BBB permeant. Any drug molecules satisfying the 'rule of five' with a bioavailability (BA) score of 0.55 are considered as sufficiently absorbable *via* oral route [29]. The bioavailability's of all the compounds are same which is 0.55. It means that all the compounds have good binding affinity and theoretically would not have any problem with oral bioavailability.

Frontier molecular orbitals (FMOs): The B3LYP/6-31G methodology was used to optimize the structures of all the compounds. Fig. 3 depicts the HOMO-LUMO energy gap of the compounds (**A-H**). Compounds **D** and **G** have a slightly lower HOMO-LUMO energy gap than the other six compounds (Table-7), which could be due to the –OEt group's electron donating tendency [21]. As a result, compounds D and G are softer than any other compounds. The hardness of an atom dictates how well it resists charge transfer to another atom or metal surface. Compounds **D** and **G** were found to have lower hardness and higher softness values than the other compounds studied. As a result, compounds **D** and **G** are found to be more reactive. Electronegativity is a chemical property that defines a molecule's proclivity to attract electrons. In present case, compound C has a high electronegative value, making it the best electron acceptor among all compounds. It could be due to the presence of chlorine atom.

Molecular electrostatic potential (MEP): Based on the electrostatic potential distribution, different shades reflect the different values of electrostatic potential at the surface; red - most electronegative electrostatic potential, blue-most positive electrostatic potential and green-zero potential [22,30]. For all *N*-aryl amides derivatives (**A-H**), it is found that the more negative electrostatic potential is around the carbonyl oxygen, yellow colour in C-N represents medium negative electrostatic potential, whereas more positive electrostatic potential is found around the pyridopyrimidine ring at the first position. Hydrogen atoms connected to heterocyclic rings have zero potential (Fig. 4).

Mulliken charge analysis: Fig. 5 depicts the Mulliken charge values for the constituent atoms of the examined molecules. The hydrogen and chlorine atoms in the molecule are positively charged and referred to as donors, whereas carbon and other atoms are negatively charged and referred to as acceptors. The hydrogen atom nearest the oxygen atom has the most positive charge [30]. This is because oxygen atoms are electro-

TABLE-6
ADME PARAMETERS OF SYNTHESIZED COMPOUNDS (**A-H**)

Compd.	MW g/mol ≤ 500	RB ≤ 10	NHA ≤ 10	NHB ≤ 5	MR	TPSA (Å^2)	C log P ≤ 5	log S	GI absorption	BBB	P-gp	CYP1A2 inhibitor	log k$_p$ (cm/s)	Drug lineness (Lipinski violation)	Bioavailability score
A	297.29	3	3	1	81.51	63.46	1.42	Soluble	High	Yes	No	Yes	-7.36	Yes	0.55
B	293.32	3	3	1	86.47	63.46	1.78	Soluble	High	Yes	No	Yes	-7.19	Yes	0.55
C	313.74	3	3	1	86.52	63.46	2.03	Soluble	High	Yes	No	Yes	-7.13	Yes	0.55
D	309.32	4	4	1	88.00	72.69	1.43	Soluble	High	No	No	No	-7.51	Yes	0.55
E	343.38	3	3	1	103.9	63.46	2.58	Soluble	High	Yes	No	Yes	-6.92	Yes	0.55
F	307.35	3	3	1	91.44	63.46	2.01	Soluble	High	Yes	No	Yes	-7.34	Yes	0.55
G	323.35	4	4	1	92.96	72.69	1.67	Soluble	High	No	No	No	-7.71	Yes	0.55
H	327.76	3	3	1	91.48	63.46	2.18	Soluble	High	Yes	No	Yes	-7.27	Yes	0.55

TABLE-7
GLOBAL REACTIVE PARAMETERS CALCULATED FOR COMPOUNDS (**A-H**)

Parameters	**A**	**B**	**C**	**D**	**E**	**F**	**G**	**H**
E_{HOMO} (eV)	-0.20350	-0.19704	-0.21166	-0.18714	-0.19063	-0.19565	-0.18569	-0.21023
E_{LUMO} (eV)	-0.09179	-0.09064	-0.09728	-0.09013	-0.09057	-0.08840	-0.08810	-0.09497
Energy gap (Δ) (eV)	0.11171	0.1064	0.11438	0.09701	0.10006	0.10725	0.09759	0.11526
Ionization energy (I) (eV)	0.20350	0.19704	0.21166	0.18714	0.19063	0.19565	0.18569	0.21023
Electron affinity (A) (eV)	0.09179	0.09064	0.09728	0.09013	0.09057	0.08840	0.08810	0.09497
Electronegativity (χ)	0.147645	0.14384	0.15447	0.138635	0.1406	0.142025	0.13689	0.1526
Chemical potential (μ) (eV)	-0.147645	-0.14384	-0.15447	-0.138635	-0.1406	-0.142025	-0.13689	-0.1526
Global hardness (η) (10^1eV)	0.55855	0.532	0.5719	0.48505	0.5003	0.53625	0.48795	0.5763
Global softness (S) (eV^{-1})	1.7903	1.87970	1.74855	2.06164	1.99880	1.86480	2.04930	1.73520
Electrophilicity index (ω) (eV)	0.19514	0.19445	0.20861	0.19812	0.19757	0.18808	0.19200	0.20204
Dipole moment (Debye)	9.6374378	9.1350752	12.72428	9.0303144	10.710887	9.8954162	9.955893	13.509229

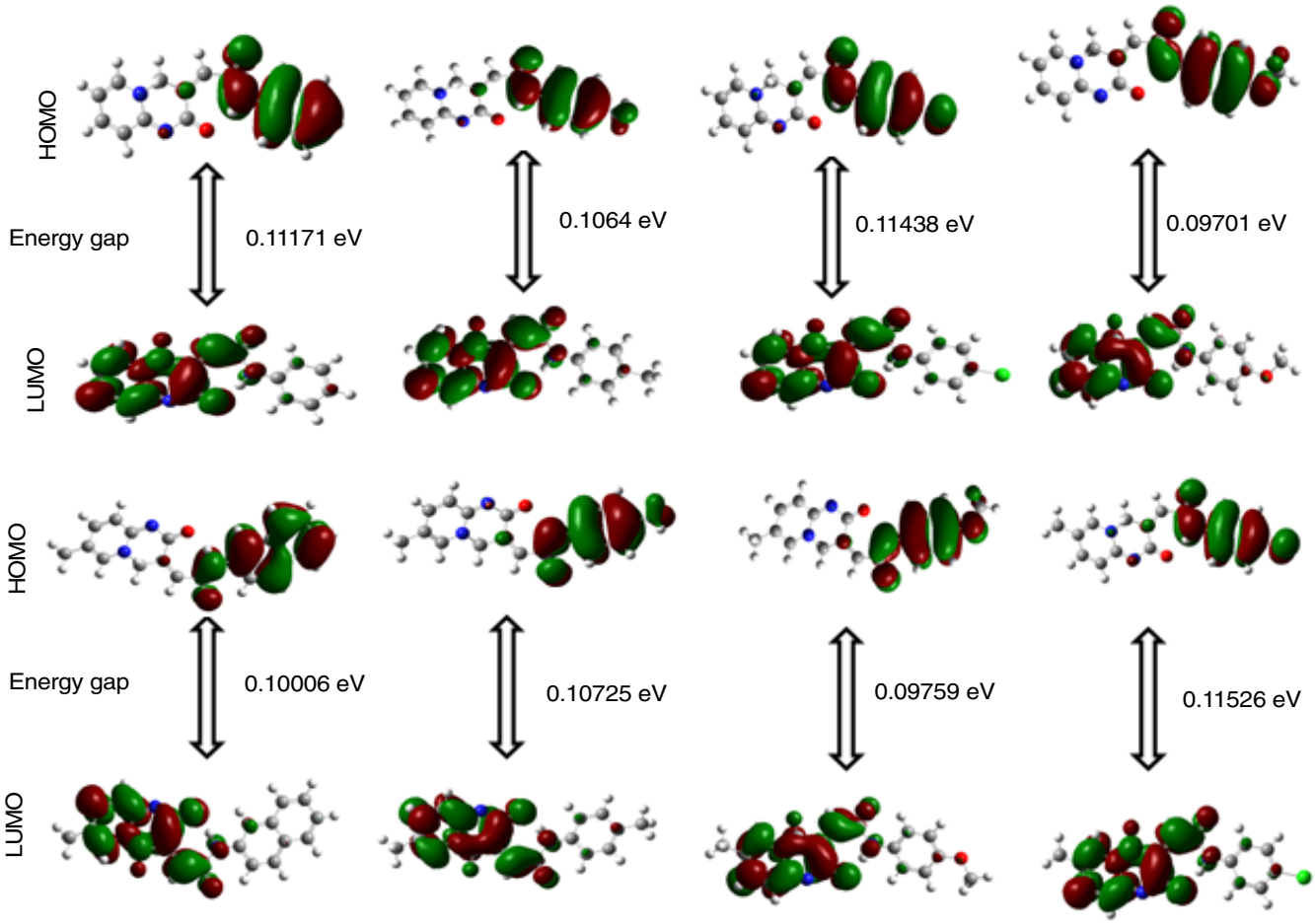

Fig. 3. HOMO and LUMO structure of the compounds (**A-H**) generated from B3LYP method using 6-31G basis set

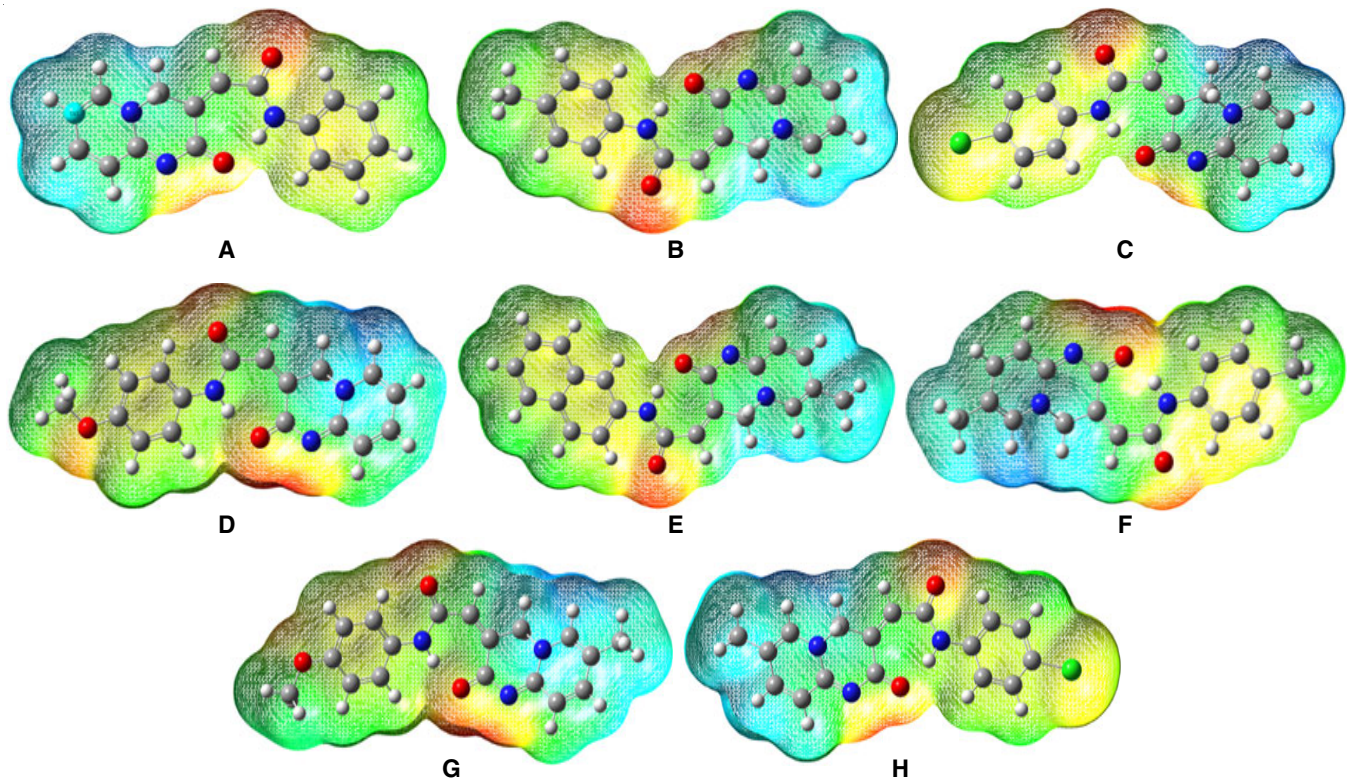

Fig. 4. Molecular electrostatic potential (MEP) of compounds (**A-H**)

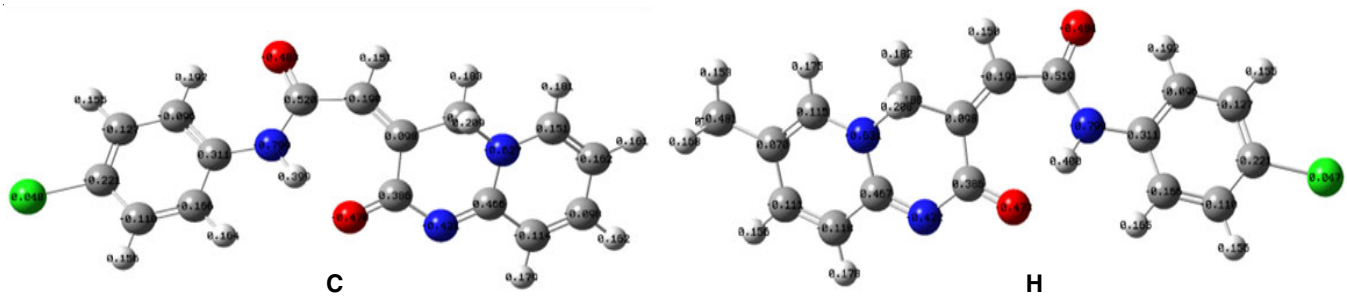

Fig. 5. Mulliken charge values for compounds **C** and **H** with positively charged chlorine atom

negative. The distribution of partial charges on the skeleton atoms indicates that electrostatic repulsion or attraction between atoms can contribute significantly to the intermolecular and intramolecular interaction estimated using the DFT/B3LYP approach.

Conclusion

The antifungal activity of *N*-aryl amides of pyrido[1,2-*a*]-pyrimidin-2-one derivatives (**A-H**) against two fungi (*Aspergillus niger* and *Candida albicans*) were investigated. Compounds **E** and **C** have strong antifungal action against *A. niger* and *C. albicans*, while other compounds exhibited significant anti-fungal activity. Computational analysis and molecular docking with probable receptors or prediction of bioactivity score and physico-chemical attributes can be used to predict the total activity spectrum of biologically active substances. Compound E showed the highest docking binding energy against target receptors 1KS5 and 1NMT in docking findings, indicating a solid agreement between docking studies and antifungal activity results. Moreover, the MEP, Mulliken charge distribution and Fukui functions were also calculated in order to identify the nucleophilic and electrophilic approaches. Furthermore, the HOMO-LUMO energy gap for compounds **D** and **G** were slightly lower in comparison to the other six compounds, which could be due to the electron donating tendency of –OEt group present. Pharmacophore calculations, such as ADME, BBB, and toxicity, were also performed and all the *N*-aryl amides of pyrido[1,2-*a*]-pyrimidin-2-one derivatives demonstrated drug-like characteristics. According to the AMDET study, all *N*-aryl amides of pyrido[1,2-*a*]-pyrimidin-2-one derivatives (**A-H**) are non-carcinogenic, low toxic and water soluble. The drug-likeness investigation demonstrated that the tested compounds (**A-H**) show promising results, indicating that the examined molecules can be employed as an intermediate in numerous drug synthesis.

CONFLICT OF INTEREST

The authors declare that there is no conflict of interests regarding the publication of this article.

REFERENCES

1. M. Ivanov, A. Ciric and D. Stojkovic, *Int. J. Mol. Sci.*, **23**, 2756 (2022); https://doi.org/10.3390/ijms23052756
2. F. Buron, J.Y. Mérour, M. Akssira, G. Guillaumet and S. Routier, Eur. J. Med. Chem., 95, 76 (2015); https://doi.org/10.1016/j.ejmech.2015.03.029
3. T. Sasada, F. Kobayashi, N. Sakai and T. Konakahara, *Org. Lett.*, **11**, 2161 (2009); https://doi.org/10.1021/ol900382j
4. R. Qingyun, T. Xiaosong and H. Hongwu, *Curr. Org. Synth.*, **8**, 752 (2011); https://doi.org/10.2174/157017911796957366
5. K.N. Kumar, K. Sreeramamurthy, S. Palle, K. Mukkanti and P. Das, *Tetrahedron Lett.*, **51**, 899 (2010); https://doi.org/10.1016/j.tetlet.2009.11.127
6. O. Nagaraja, Y.D. Bodke, I. Pushpavathi and S. Ravi Kumar, *Heliyon*, **6**, e04245 (2020); https://doi.org/10.1016/j.heliyon.2020.e04245
7. M. Huo, L. Zhao, T. Wang, W. Zong and R. Liu, *J. Mol. Recognit.*, **33**, e2822 (2020); https://doi.org/10.1002/jmr.2822
8. E. Yuriev, M. Agostino and P.A. Ramsland, *J. Mol. Recognit.*, **24**, 149 (2011); https://doi.org/10.1002/jmr.1077
9. S. Venugopal, A. Anbazhagan, M. Rajeswari and S. Sundaram, *J. Indian Chem. Soc*., **97**, 1584 (2020).
10. A. Kumer and M.W. Khan, *J. Mol. Struct.*, **1245**, 131087 (2021); https://doi.org/10.1016/j.molstruc.2021.131087
11. O. Trott and A.J. Olson, *J. Comput. Chem.*, **31**, 455 (2010); https://doi.org/10.1002/jcc.21334
12. S. Forli, R. Huey, M.E. Pique, M.F. Sanner, D.S. Goodsell and A.J. Olson, *Nat. Protoc.*, **11**, 905 (2016); https://doi.org/10.1038/nprot.2016.051
13. S.A. Gandhi, R.D. Modh, U.H. Patel, B.D. Patel, K.H. Chikhalia and A.C. Patel, *Mol. Cryst. Liq. Cryst.*, **708**, 98 (2020); https://doi.org/10.1080/15421406.2020.1811023
14. S. Dacrory, A.H. Hashem and M. Hasanin, *Environ. Nanotechnol. Monit. Manag.*, **15**, 100453 (2021); https://doi.org/10.1016/j.enmm.2021.100453
15. S. Khademi, D. Zhang, S.M. Swanson, A. Wartenberg, K. Witte and E.F. Meyer, *Acta Crystallogr. D Biol. Crystallogr.*, **58**, 660 (2002); https://doi.org/10.1107/S0907444902003360
16. S.S. Meenambiga and K. Rajagopal, *J. Appl. Pharm. Sci.*, **8**, 37 (2018); https://doi.org/10.7324/JAPS.2018.8707
17. M.L. Beatrice, S.M. Delphine, M. Amalanathan and H.M. Robert, *Asian J. Chem.*, **32**, 2475 (2020); https://doi.org/10.14233/ajchem.2020.22718
18. F. Qi, Q. Qi, J. Song and J. Huang, *Chem. Biodivers.*, **18**, e2000804 (2021); https://doi.org/10.1002/cbdv.202000804
19. F. Qi, S. Wang, C. Wei, Z. Guo, J. Song and J. Huang, *Rev. Roum. Chim.*, **66**, 509 (2021); https://doi.org/10.33224/rrch.2021.66.6.03
20. F. Qi, J. Song and J. Huang, *J. Mol. Struct.*, **1224**, 129044 (2021); https://doi.org/10.1016/j.molstruc.2020.129044
21. M. B, Y.D. Bodke, N. O, L.T. N, N. G and S. Ma, *J. Mol. Struct.*, **1246**, 131170 (2021); https://doi.org/10.1016/j.molstruc.2021.131170
22. M.I. Azad, T. Khan, A.K. Maurya, M. Irfan Azad, N. Mishra and A.M. Alanazi, *J. Mol. Recognit.*, **34**, e2918 (2021); https://doi.org/10.1002/jmr.2918
23. T. Khan, S. Dixit, R. Ahmad, S. Raza, I. Azad, S. Joshi and A.R. Khan, *J. Chem. Biol.*, **10**, 91 (2017); https://doi.org/10.1007/s12154-017-0167-y

24. R. Dumpati, V. Ramatenki, R. Vadija, S. Vellanki and U. Vuruputuri, *J. Mol. Recognit.*, **31**, e2706 (2018); https://doi.org/10.1002/jmr.2706
25. H.S.N. Prasad, A.P. Ananda, T.N. Lohith, P. Prabhuprasad, H.S. Jayanth, N.B. Krishnamurthy, M.A. Sridhar, L. Mallesha and P. Mallu, *J. Mol. Struct.*, **1247**, 131333 (2022); https://doi.org/10.1016/j.molstruc.2021.131333
26. C.H. Li, H.R. Wang and T.R. Yan, *Molecules*, **17**, 9774 (2012); https://doi.org/10.3390/molecules17089774
27. A. Fatima, G. Khanum, S. Savita, K. Pooja, I. Verma, N. Siddiqui and S. Javed, *J. Mol. Liq.*, **346**, 117150 (2022); https://doi.org/10.1016/j.molliq.2021.117150
28. N. Agarwal, I. Verma, N. Siddiqui and S. Javed, *J. Mol. Struct.*, **1245**, 131046 (2021); https://doi.org/10.1016/j.molstruc.2021.131046
29. Y.C. Martin, *J. Med. Chem.*, **48**, 3164 (2005); https://doi.org/10.1021/jm0492002
30. A.M. Deghady, R.K. Hussein, A.G. Alhamzani and A. Mera, *Molecules*, **26**, 3631 (2021); https://doi.org/10.3390/molecules26123631